

Unravelling the potential of nitric acid as a surface modifier for improving the hemocompatibility of metallocene polyethylene for blood contacting devices

Muthu Vignesh Vellayappan, Saravana Kumar Jaganathan, Ida Idayu Muhamad

Design of blood compatible surfaces is obligatory to minimize platelet surface interactions and improve the thromboresistance of foreign surfaces when they are utilized as biomaterials particularly for blood contacting devices. Pure metallocene polyethylene (mPE) and nitric acid (HNO₃) treated mPE antithrombogenicity and hydrophilicity were investigated. The contact angle of the mPE treated with HNO₃ decreased. Surface of mPE and HNO₃ treated mPE investigated with FTIR revealed no major changes in its functional groups. 3D Hirox digital microscopy, SEM and AFM images show increased porosity and surface roughness. Blood coagulation assays prothrombin time (PT) and activated partial thromboplastin time (APTT) were delayed significantly ($P < 0.05$) for HNO₃ treated mPE. Hemolysis assay and platelet adhesion of the treated surface resulted in the lysis of red blood cells and platelet adherence, respectively indicating improved hemocompatibility of HNO₃ treated mPE. To determine that HNO₃ does not deteriorate elastic modulus of mPE, the elastic modulus of mPE and HNO₃ treated mPE was compared and the result shows no significant difference. Hence, the overall observation suggests that the novel HNO₃ treated mPE may hold great promises to be exploited for blood contacting devices like grafts, catheters, and etc.

1 **Unravelling the potential of nitric acid as a surface modifier for improving the**
2 **hemocompatibility of metallocene polyethylene for blood contacting devices**

3

4 Muthu Vignesh Vellayappan¹, Saravana Kumar Jaganathan^{1*}, Ida Idayu Muhamad¹

5 ¹ IJN-UTM Cardiovascular Engineering Centre, Faculty of Biosciences and Medical
6 Engineering, Universiti Teknologi Malaysia, Johor Bahru 81310, Malaysia

7 ***Corresponding author:** Dr Saravana Kumar Jaganathan, IJN-UTM Cardiovascular
8 Engineering Centre, Faculty of Biosciences and Medical Engineering, University Teknologi
9 Malaysia, Johor Bahru 81310, Malaysia; Email: jaganathaniitkgp@gmail.com; Tel; 00607-
10 5558548; Fax: 07-5558553

11 **Abstract**

12 Design of blood compatible surfaces is obligatory to minimize platelet surface
13 interactions and improve the thromboresistance of foreign surfaces when they are utilized as
14 biomaterials particularly for blood contacting devices. Pure metallocene polyethylene (mPE) and
15 nitric acid (HNO₃) treated mPE antithrombogenicity and hydrophilicity were investigated. The
16 contact angle of the mPE treated with HNO₃ decreased. Surface of mPE and HNO₃ treated mPE
17 investigated with FTIR revealed no major changes in its functional groups. 3D Hirox digital
18 microscopy, SEM and AFM images show increased porosity and surface roughness. Blood
19 coagulation assays prothrombin time (PT) and activated partial thromboplastin time (APTT)
20 were delayed significantly ($P < 0.05$) for HNO₃ treated mPE. Hemolysis assay and platelet
21 adhesion of the treated surface resulted in the lysis of red blood cells and platelet adherence,
22 respectively indicating improved hemocompatibility of HNO₃ treated mPE. To determine that
23 HNO₃ does not deteriorate elastic modulus of mPE, the elastic modulus of mPE and HNO₃
24 treated mPE was compared and the result shows no significant difference. Hence, the overall
25 observation suggests that the novel HNO₃ treated mPE may hold great promises to be exploited
26 for blood contacting devices like grafts, catheters, and etc.

27 **Keywords:** Nitric acid, hemocompatibility, surface modification, blood contacting device.

28 **Introduction**

29 The surface modification of biomaterials is a process of modifying its surface properties
30 by changing its inherent physical, chemical or biological properties to possess desirable
31 characteristics (John et al, 2015). Generally, the surface modification of biomaterials can be done
32 via different techniques for the biocompatibility enhancement, which is the cornerstone property
33 required whilst selecting a blood contacting device (Jaganathan et al, 2014a; Vellayappan et al,
34 2015a). There is a wide range of blood contacting devices available nowadays like grafts,
35 catheters, hemodialysis, bypass/extracorporeal membrane oxygenation, and ventricular assist
36 devices (VADs). Even though there is a widespread need for blood contacting devices, the
37 formation of blood coagulation as well as commencement of thrombotic events whilst the
38 biomaterial comes in contact with the blood, remains as a daunting challenge for researchers to
39 decipher (Velayyappan et al., 2015). A recent statistic shows that 65-88% of aortic repair
40 procedures performed in the US are being replaced with endovascular grafts and the thrombus
41 formation in aortic side branches often leads to ischemia (Thompson, 2013). Another clinical
42 study dictates that thrombus formation on the catheter surface in 50% of patients undergoing
43 diagnostic angiography (Formanek G & Frech RS., 1970). Moreover, thrombosis are found to be
44 the precipitating event in 30-40% of central venous catheter malfunctions (Vascular Access,
45 2006). Thus, prevention of thrombotic deposition and occlusion, triggered by the activation of
46 the coagulation cascade and platelets, is a mandatory property which the implanted blood
47 contacting devices should possess before it is recommended for clinical trials.

48 The advent of latest technology has paved the way for the discovery of novel polymers
49 like metallocene which is a new class of polyolefins with superior performance characteristics
50 like improved toughness, sealability, clarity, and elasticity. Metallocene is made up of two

51 cyclopentadienyl anions (Cp,) which are attached to a metal center (M) with an oxidation state II,
52 hence resulting in a general formula $M(C_5H_5)_2$ (Kealy TJ & Pauson PL, 1951). The metallocene
53 polyethylene (mPE) is one of the versatile polymers. The mPE has wide spectrum of applications
54 in disposable bags, storage bottles, blood bags, and syringe tubes. Albeit mPE has an excellent
55 permeability to oxygen and functions as an effective barricade towards ammonia and water, yet
56 mPE poor blood compatibility hampers it from being used for blood contacting devices
57 (Mohandas et al, 2013). Thus, different works were done for enhancing the blood compatibility
58 of mPE recently to promote it for various biomedical applications.

59 In our group, we are exploring several modification techniques to improve the blood
60 compatibility of mPE. Recently, Mohandas et al., utilized microwave radiation for surface
61 modification of the mPE to improve its blood compatibility (Mohandas et al, 2013).
62 Furthermore, the effect of hydrochloric (HCl) acid treatment on the metallocene polyethylene
63 mPE depicted an enhanced blood compatibility of mPE compared to the untreated mPE sample
64 (Jaganathan et al, 2014).

65 Since the HCl etching effect on mPE yielded good results, it further motivated us to find
66 other available substitutes which are cost effective and easily available for improving the blood
67 compatibility of mPE. Thus, being a very strong acid and oxidizing agent, we have selected
68 HNO_3 for improving the blood compatibility of mPE. In a work done utilizing HNO_3 by
69 Moreno-Castilla et al., dictates that the HNO_3 treatment affects the surface area of activated
70 carbons and their porosity the most compared to the other treatments like hydrogen peroxide, and
71 ammonium peroxydisulfate treatments (Moreno-Castilla et al, 1995). Moreover, Dong et al.,
72 demonstrated the HNO_3 oxidation treatment on CNT modifies the CNTs physical and chemical
73 properties resulting in improved CNTs biocompatibility (Dong et al, 2012). For the first time the

74 effect of HNO₃ treatment on mPE is documented in this work. Furthermore, the present study is
75 done to ascertain the modifications induced in mPE and its impact on the blood compatibility of
76 the HNO₃ treated mPE samples.

77 **Materials and Methods**

78 **Ethics Statement**

79 The blood coagulation assays were carried out in India and the characterization tests were
80 done in Malaysia. Prior to blood procurement, the written consent form was given to the healthy
81 volunteers. They read the benefits and risks of participation before expressing his/her willingness
82 by signing the form. All protocols of blood procurement and consent procedure were approved
83 by the Pacheri Sri Nallathangal Amman (PSNA) College of Engineering and Technology Ethical
84 Committee of Dindigul with an approved IRB number: H30114. Later, the blood was extracted
85 via venipuncture from aspirin-free healthy adult human donor and it is prevented from
86 coagulation with trisodium citrate at a volumetric ratio of 9:1. Newly prepared platelet rich
87 plasma (PRP) was acquired from the Dindigul Blood Bank, Dindigul, India.

88 **Sample Preparation and Acid Treatment**

89 Initially, two mPE films of dimensions 10 cm × 10 cm were cut into two samples with a
90 size of 1 cm × 1 cm. Then the samples were washed with 70% ethanol and distilled water prior
91 subjecting it to HNO₃ treatment. Prior to HNO₃ treatment, the mPE samples were washed with
92 70% ethanol, then was rinsed in distilled water to remove any impurities present on the surface
93 of the sample. Then, 8- 10 ml of concentrated HNO₃ with molarity of 15.9M was poured into
94 petri dish which contains the square shaped sheets of mPE. The acid and sample containing
95 dishes were later placed on the rocking shakers which moves at a constant speed. Moreover, in
96 this work mPE sample were subjected to HNO₃ exposure for the different time durations. From

97 that, the optimized timings were selected by observing surface changes with an optical
98 microscope at 40x. The samples subjected for a lesser duration didn't confer notable surface
99 modifications when compared with control, however, during 30 minutes of exposure significant
100 change in the surface of mPE was observed. While subjecting samples for a prolonged period,
101 changes noted, were not significant compared to 60 minutes treated sample. Thus, for
102 characterization studies, 30 minutes and 60 minutes treated samples alone were considered. Once
103 the acid treatment was done, the samples were washed in distilled water and dried at room
104 temperature overnight before performing any characterization tests. Whilst preparing the samples
105 for blood compatibility tests, samples were kept in a beaker with physiological saline and then in
106 a rotary shaker overnight at 37°C to remove the acid present on the surface of the polymer.

107 The scheme of the experiments performed was shown in Figure 1.

108 **Characterization of the Samples**

109 **Contact Angle Measurement**

110 The hydrophilicity tendency of the polymer was determined using Dynamic Contact
111 Angle Analyzer (FTA200—First Ten Angstroms). Here, water droplet was placed on the surface
112 of the sample. Water droplet of 1 μL was used and the photographs were taken in the ultra-fast
113 mode within 30 seconds. The degree of the angle formed is determined using computer
114 interfaced software. The contact angles were recorded and analyzed for the samples which are
115 not treated with HNO_3 and 30min and 60min HNO_3 exposed samples ($n = 3$).

116 **Attenuated Total Reflectance Fourier Transfer Infrared Spectroscopy (ATR-FTIR)**

117 ATR-FTIR equipment NEXUS- 870 model spectrophotometer was utilized have
118 additional features such as extended beam splitter, two light sources, and middle band MCT
119 detectors with various sampling options. This was used for the purpose of analyzing the chemical

120 compositions or functional groups present within the polymer. There were three samples present
121 in the study, which are untreated and 30 min and 60min HNO₃-treated samples. All these
122 samples were studied using this ATR-FTIR.

123 **3D-Hirox Digital Microscope**

124 The latest 3D-Hirox digital microscope model (KH-8700) was used to determine the
125 formation of pits and pores of the samples. The 3D-Hirox digital microscopy images are very
126 useful in determining the morphological structure of samples to determine whether the sample
127 has pores or it has an even surface. There are two types of images which are obtained from 3D-
128 Hirox digital microscopy either with or without profilometry line. The surface morphology of
129 1cm x 1cm of mPE and HNO₃ treated mPE sample was assessed at an area of approximately
130 5757μ² at a magnification of 500X. The same as white light confocal profilometry, in-focus and
131 3D images were obtained using this 3D microscope. Slices of the image were captured at
132 different heights acquired for the surface topography analysis (Pereira et la, 2013). Maximum of
133 three profiling lines is chosen as the profiling value of the each sample. Each point in X, Y and Z
134 axes of the profiling line is measured and their values can be exported in excel sheet to represent
135 the height of the pits in the sample. Data processing was performed using the in-build 3D
136 profilometry software. Images were recorded at standard 1,200 to 1,600 pixel resolution.

137 **Scanning Electron Microscope**

138 The surface microstructure of the samples can be critically analyzed in detail by using
139 SEM. The SEM which is utilized to study the polymeric samples was JEOL JSM5800 SEM with
140 OXFORD ISI 300 EDS X-ray Microanalysis System. All samples underwent gold sputtering and
141 then been studied using SEM at a magnification of 1500x.

142

143 Atomic Force Microscopy

144 The surface roughness of the samples can be determined with the help of AFM. The
145 AFM model used to analyze the samples is SPA300HV with a scan rate of 1.502 Hz in tapping
146 mode. Here, the surface morphology of mPE and HNO₃ treated mPE sample was measured by
147 AFM in contact mode on a 10 × 10 μm² area, and the mean average surface roughness (Ra) and
148 3D pictographic view is obtained. Each AFM image was analyzed in terms of Ra (Pelagade et al,
149 2012). The surface roughness is calculated using the software SPIWin.

150 Tensile Testing

151 The tensile strength was tested using ZWICK Universal Tester (Z010, Germany) at a
152 gage length of 15 mm and a speed of 10 mm⁻¹ for all the specimens at a load cell capacity of 100
153 N with a sample thickness of 1mm. The reported tensile moduli is represented as average results
154 of five tests.

155 Blood Coagulation Assays**156 Prothrombin Time (PT)**

157 Prothrombin time is a valuable indicator to find the prohibition of extrinsic pathway.
158 Platelet poor plasma (PPP) (100 μL at 37°C) was applied on untreated and treated polymer
159 surface with NaCl-thromboplastin (Factor III, 100 mL, Sigma) which contains Ca²⁺ ions. The
160 time consumed for the formation fibrin clot was assessed with the help of a stopwatch and a steel
161 hook (*n* = 3) (Amarnath LP, Srinivas A and Ramamurthi A et al, 2006).

162 Activated Partial Thromboplastin Time (APTT)

163 APTT is utilized for studying the propensity of the blood to coagulate via intrinsic
164 pathway and to determine the effect of biomaterial on delaying the process. Platelet poor plasma
165 (100 μL at 37°C) is incubated in prior with substrates at 37°C and followed by its activation by

166 adding rabbit brain cephalin (100 μ L 37°C). Later, the samples were incubated at 37°C for 5min
167 and followed by incubation with calcium chloride (0.025M). Inclusion of CaCl₂ triggers the
168 clotting process. The time taken from the inclusion of CaCl₂ up to clot formation is recorded as
169 the activated partial thromboplastin time (APTT) ($n = 3$) (Amarnath LP, Srinivas A and
170 Ramamurthi A et al, 2006).

171 **Hemolysis Assay**

172 The HNO₃ treated (30min and 60min) and untreated samples were equilibrated with
173 physiologic saline (0.9%w/v; 37°C, 30 min) followed by its incubation with 3mL aliquots of
174 citrated blood diluted with saline (4 : 5 ratios by volume). This mixture of blood and distilled
175 water was prepared at a ratio of 4: 5 by volume to result in comprehensive hemolysis which was
176 used as the positive control. Physiological saline solution was utilized as negative control which
177 produces no coloration. The samples were subjected to incubation in their respective mixtures
178 (60min, 37°C). These mixtures were later centrifuged and their absorbance of clear supernatant
179 was determined at 542 nm. The absorbance of positive control was normalized to 100% and the
180 absorbance of both the samples was ascertained as a percentage of hemolysis whilst comparing it
181 with positive control ($n = 3$) (Amarnath LP, Srinivas A and Ramamurthi A et al, 2006).

182 **Platelet Adhesion Assay**

183 The samples were subjected to HNO₃ exposure for 60 min and later incubated along with
184 physiological saline 0.9%w/v; 37°C, 30 min) . This is kept on the rotary shaker for an hour to
185 wash of the acid residues on the surface of the polymer. This is followed by immersing of treated
186 and untreated samples in 1mL fresh PRP and the incubation was maintained at 37°C for an hour.
187 PRP was poured off and the membranes were rinsed in physiologic saline and dried. Ultimately,
188 the samples were viewed using the microscope ($n = 3$). The polymer surface was photographed

189 and platelet count was determined on a region with a 40x magnification (Amarnath LP, Srinivas
190 A and Ramamurthi A et al, 2006).

191 **Statistical Analyses**

192 All experiments were conducted thrice independently. One-way ANOVA was done to
193 determine statistical significance. The results obtained from all experiments are expressed as
194 mean \pm SD. In case of qualitative experiments, a representative of three images is shown.

195 **Results**

196 The mean contact angle of the control was found to be 86.06°. This was found to be far
197 greater in comparison to the acid treated samples. The mean contact angles of 30 and 60 min
198 treated samples are 72.03° and 69.73°, respectively, were significantly lower with respect to
199 untreated surface as shown in (Table 1).

200 FTIR was performed for the determination of chemical composition of untreated and
201 treated samples as shown in Figure 2. No changes were observed in the functional groups
202 between the treated and the untreated ones. There were alike peaks observed at wavelengths
203 2850 cm^{-1} and 2930 cm^{-1} belonging to the alkane group (C–H stretch). The peaks were also
204 found at 1647 cm^{-1} (C=C bending), 1470 cm^{-1} (C–H bending) and at 725 cm^{-1} (C–H rocking),
205 belonging to the alkane family but differing in their structures. A peak was also observed at 1020
206 cm^{-1} which belongs to the C–O stretching. Nevertheless, the intensity of the peaks associated
207 with the treated surface was observed to slightly differ from untreated one.

208 The morphological analysis of the samples was done using the 3D Hirox Microscopy and
209 SEM where as the nanotopographic analysis of the sample was performed with the help of AFM.
210 The images obtained are shown in Figure 3(a)-(f). Figure 3(a) represents the 3D image of the
211 control and Figure 3(b) shows its profiling image. Likewise, the Figure 3 (c) and Figure 3(d)

212 depict the 3D image and its profiling image of the thirty minutes HNO_3 treated sample,
213 respectively. Similarly, Figure 3(e) and 3(f) elucidates the 3D image and its profiling image of
214 one hour HNO_3 treated mPE sample. The graph plotted with the values obtained from the 3D-
215 Hirox digital microscope is represented in Figure 4. Here, each point in the profile line is
216 measured and computed. These points represent the height of the pits in mPE surface. Thus, in
217 Figure 4, the height of the pits or pores is plotted against the area of the profile line. From this
218 graph, it is palpable that there is less number of pores of pits in case of the control mPE. It is
219 found that the number of pores, increased in the 30 minutes and found to be highest in 1 hour
220 acid treated mPE sample. The 1 hour HNO_3 treated sample has the maximum number of pores
221 with greater depth of fissures and holes which was ascertained using the 3D profiling. Figure 4
222 shows the depth of the pores formed due to the etching effect of the HNO_3 and it is evident that
223 the control has the least pore depth, followed by 30 minutes HNO_3 treated sample and finally the
224 one hour HNO_3 treated sample. Hence, the duration of acid treatment has an impact on the
225 surface porosity by affecting the pore diameter or area. From the Fig. 4, it is visible that $42.5\mu\text{m}$
226 was the highest height of the pore in the case of one 1 hour HNO_3 treated sample where the
227 highest pore for the 30 minutes HNO_3 treated mPE was $30\mu\text{m}$ and $17.5\mu\text{m}$ for untreated mPE.
228 This shows the numerical values, data on relative changes for clearly differentiating the etching
229 effect of HNO_3 on mPE.

230 SEM imaging is another surface characterization method of the samples at the micro
231 level (Zhao et al, 2011). Topography of the polymers was investigated and morphological studies
232 of the polymer samples were made Fig. 5(a),(b) and (c). It was observed that the surface of mPE
233 sample has very less or negligible pits under a 1500x magnification. However, on observing the
234 SEM image of 30 minutes treated sample, it was found that the surface of the treated samples has

235 been etched by the acid exposure. A few number of pit formation was also observed. Moreover,
236 the size and the number of the pits seems to increase in case of the 60min acid treated sample.

237 The AFM images are represented in Fig. 5 (d) and (e). Fig. 5(d) is the AFM image of the
238 untreated mPE sample and Fig. 5(e) is the AFM image of one hour HNO₃ treated mPE sample.
239 From the results obtained, it was found that the mean value of Ra of untreated mPE film and 1
240 hour HNO₃ treated mPE surface are 2.069 and 5.127 nm, respectively. The nanotopographic
241 analysis of the samples was performed using AFM. Fig. 5(d) illustrates the 3D surface
242 topography of the sample mPE. Here, it is observed that the surface of the sample is even with
243 less hills and valley structures in the sample. On the other hand Fig. 5(e) which is the 1 hour
244 HNO₃ treated sample AFM image shows more number of hill and valley structure on the surface
245 of the sample.

246 The average tensile testing result of mPE before and after nitric acid treatment is
247 represented in Fig. 6. From the tensile stress-strain curve it is palpable that the elastic modulus of
248 HNO₃ treated mPE (34.75MPa) is slightly greater than the elastic modulus of untreated mPE
249 (31.32MPa). The elastic modulus, maximum force, elongation at maximum force and work up to
250 maximum force is given in table 2.

251 Prothrombin time and activated partial thromboplastin time tests were done on the three
252 samples, namely, untreated and 30min and 60min HNO₃ treated. Their results of PT and APTT
253 were summarized in Fig. 7(a) and Fig. 7(b), respectively. Both PT and APTT demonstrated an
254 increase in their value for acid treated samples compared to the control. Mean PT of untreated
255 sample was observed to be 19.23 s, whereas 30 and 60min HNO₃ exposed samples shown 19.86
256 s and 21.4 s, respectively. Likewise, mean APTT was found to be 105.66 s, 113 s and 136.33 s
257 for untreated, 30 min and 60 min acid treated mPE, respectively. Statistical analysis of the

258 untreated sample with the treated ones using one-way ANOVA insinuates significant differences
259 ($P < 0.05$) between them for both PT and APTT times after 60 min exposure.

260 Besides that, hemolysis is an important screening test, which provides quantification of
261 small levels of plasma hemoglobin that may not be assessed under in vivo conditions (Schopka
262 et al, 2010). The hemolysis test was conducted on treating samples and untreated sample for
263 investigating the effect of polymer surface on red blood cells (RBC). Mean absorbance seemed
264 to decrease in the case of treated samples (0.02 and 0.007 for 30min and 60min HNO₃-treated
265 samples) compared with the untreated (0.05) mPE, indicating lesser damage incurred and
266 interaction between the treated samples and RBC Fig. 7(c). This is because the absorbance is
267 directly proportional to the hemolytic index (HI) of the RBC. Statistical analysis of the untreated
268 as well as acid treated samples (absorbance at 542nm) using one-way ANOVA ascertained
269 significant differences ($P < 0.05$) between them after 30 and 60min treatment. From the results
270 obtained, it is obvious that the 1 hour HNO₃ treated mPE is the least hemolytic compared to other
271 samples. Moreover, it was also found that an absorbance value of 1 hour HNO₃ treated mPE to
272 be in similar trend compared to the one hour HCl treated mPE (Jaganathan et al, 2014).

273 Besides HI, the adhesion of platelets on a blood contacting device's surface could result
274 in coagulation and thrombus formation. Hence, the platelet adhesion test has to be performed to
275 analyze the blood compatibility of blood contacting device (Wenzhong et al, 2008). The number
276 of platelets adhered to a surface of treated polymers was found to be reduced to a great extent
277 compared to the number of platelets which was found in the untreated sample. A maximum of 22
278 platelets was observed on the surface of the untreated samples, meanwhile the number of
279 platelets decreased to a maximum of 15 platelets on 60min treated samples as represented in Fig.
280 8(a). Statistical analysis of the untreated sample with the treated one (number of platelets

281 adhered) with one-way ANOVA shown significant differences ($P < 0.05$) between them after 60
282 min treatment. The image of the polymer surface further dictates the decrease in the number of
283 platelets adhered on the acid treated present in Fig. 8 (b) compared to the untreated polymer
284 surfaces as shown in Fig. 8(c).

285 Discussion

286 Blood clotting occurs when blood comes in contact with a foreign surface such as
287 implants following platelet activation. This can be catastrophic in clinical settings, especially in
288 case of various biomedical applications like grafts, catheters, hemodialysis,
289 bypass/extracorporeal membrane oxygenation, and ventricular assist devices (Qi, Maitz &
290 Huang, 2013). In order to circumvent this issue, the hemocompatibility of the blood contacting
291 devices has to be improved and HNO_3 surface treated mPE holds a great potential. For
292 ascertaining the topographical modification caused by HNO_3 on the mPE sample,
293 characterization tests was performed using 3D Hirox, SEM, AFM, contact angle and FTIR. On
294 the other hand, the blood compatibility of the sample was studied by conducting different blood
295 coagulations assays like hemolysis assay, PT, APTT, and platelet adhesion.

296 The decrease in contact angle indicates the improved wettability and hydrophilicity of the
297 mPE polymer. It is a well known fact that the surface energy is a vital parameter determining
298 polymer's adhesion, material wettability and even biocompatibility (Kwok, Wang & Chu PK,
299 2005). Thus, the assessment of contact angles is contemplated as one of the most convenient
300 method for the determination of surface free energy of solid samples. This technique depends on
301 the interactions between the solid sample of interest as well as liquids with well determined
302 surface tensions. Our result is in good agreement with our previous published results of HCl
303 exposed mPE (Jaganathan et al, 2014). Furthermore, in a recent work, Gomathi et al., had

304 performed surface modification of polypropylene by nitrogen containing plasma improved the
305 polymer's wettability by decreasing the water contact angle and resulted in enhanced
306 biocompatibility and blood compatibility further corroborates our results (Gomathi et al, 2012).
307 According to Wenzel model, the improvement in the surface roughness of mPE contributes to
308 the reduction in the water contact angle of mPE (Chau et al, 2009). Thus, it indirectly shows that
309 the surface roughness of the mPE sample are improved by the HNO₃ treatment, thereby
310 decreasing the contact angle. Ultimately, the hydrophilicity and mPE hemocompatibility is
311 improved where it can serve as a putative blood contacting device (Zhao et al, 2011).

312 The intensity of absorption was found to be improved with respect to all peaks in the acid
313 treated mPE. These observations insinuate that there are modifications in the surface
314 morphology. There is no alteration in the functional groups of the treated and untreated samples
315 which is done by Attenuated Total Reflectance Fourier Transform Infrared Spectroscopy (ATR-
316 FTIR) studies. However, the variation in the intensity of the peaks depicts that there is some
317 morphological changes occurred. Hence, this elucidates that there is no change in the functional
318 groups in mPE surface, even after HNO₃ treatment of mPE which is similar to our HCl exposed
319 mPE (Jaganathan et al, 2014). Thus, HNO₃ treated mPE sample would have enhanced blood
320 compatibility without affecting the chemical structure of mPE since the surface roughness of the
321 mPE is increased by the HNO₃ treatment rather than modifying the chemical structure of mPE.
322 The percentage of weight loss study was also performed, but the change in the weight of the
323 sample after HNO₃ treatment was not significant which ascertains there is no strong oxidation
324 have occurred to increase the weight of the HNO₃ treated mPE samples (result not shown). This
325 is in accordance with the FTIR result which didn't show appreciable changes in surface
326 functional groups. Thus, it can be elucidated as the improved surface roughness resulted in better

327 hydrophilicity and hemocompatibility of HNO_3 treated mPE rather than the change induced in
328 the sample surface functional group by HNO_3 treatment.

329 The 3D Hirox Microscopy images can be interpreted as HNO_3 etches the surface of mPE,
330 and one hour acid treatment must have etched the mPE surface more than the 30 minutes treated
331 sample, thereby resulting in mPE with more pits and pores with higher depth compared to the
332 control. These observations can be compared to a later work of Vital et al., where the amplitude
333 of depressions formed in the surface of polymer increased after tetrahydrofuran (THF) and acetic
334 acid surface treatment whereas thickness of the polymer film remained unchanged (Vital et al,
335 2015). Hence, the etching effect of the acid has a favorable impact on the final surface
336 wettability of the polymer, thereby making it more hydrophilic similar to the other surface
337 treatments like plasma treatment to make it blood compatible for various blood contacting device
338 applications (Yue et al, 2014).

339 Similarly, a larger surface disorientation and improved surface roughness were noticed in
340 60 min treated sample using SEM images. The SEM images of a recent study show the
341 morphology of isotactic polypropylene (IPP) surfaces of Argon plasma treatment, showing
342 amorphous region is etched on the surface of IPP and the etching depth was found to be
343 increasing with an increase in the time of plasma treated thereby improving its biocompatibility
344 (Ma et al, 2011). Likewise, SEM images of the treated and untreated samples to clearly show
345 that there are pits formed in the surface of the mPE polymer when it is treated with HNO_3 and the
346 pit size is also increased with the increase in the time of acid treatment. Since pits were formed,
347 the morphological characteristic such as roughness was also observed to be increased in case of
348 the HNO_3 treated samples. It is obvious from the Fig. 5 that the number of pits formed in the

349 sample is in the descending order of 60minutes HNO₃, 30minutes HNO₃ and then finally the
350 control.

351 It was found that the Ra value of the 1 hour HNO₃ treated sample value is almost twice
352 greater than the control. This is because of more number of hills and valley nano-topographic
353 structure in the mPE sample resulted due to the etching effect of the HNO₃ on the mPE sample.
354 This result is found to be similar to a latest study done by Cesca et al., where the AFM result
355 obtained after poly-3-caprolactone (PCL) etched using mixed gas SF₆/Argon at -5°C has an
356 improved surface roughness resulting in improved biocompatibility (Cesca et al, 2014). The
357 roughness values obtained using AFM also evidenced the surface structuring after subjecting the
358 sample to surface modification techniques to produce a rougher surface (Tverdokhlebov et al,
359 2014; Wanke et al, 2014). Similarly, there were other studies carried out show increase in surface
360 roughness of sample results in improved biocompatibility (Slepicka et al, 2013). Hence, AFM
361 nano imaging further bolsters the concept of nanotopographic surface modification caused by the
362 acid etching effect on mPE analyzed using Hirox microscopy and SEM. This formed
363 nanotopographic surface result in improved wettability and hydrophilicity ascertained by contact
364 angle analysis, thereby improving the blood compatibility of mPE which is the cornerstone for
365 blood contacting devices.

366 Since nitric acid improves porosity and blood compatibility of mPE, the elastic modulus
367 of mPE was studied to make sure that the nitric acid treatment does not deteriorate the elastic
368 modulus of mPE. There was no significant change was observed and minor improvement in the
369 elastic modulus of HNO₃ treated mPE which may have resulted due to increase in the roughness
370 of the surface in mPE. This result is in accordance with a recent study where the impact strength
371 of nitric acid treated polyoxymethylene improved compared to those untreated samples (Zhang et

372 al, 2014). The surface of the carbon fibers synthesized from polyacrylonitrile was subjected to
373 HNO₃ treatment and it was found that the tensile strength of the fibers increased compared to
374 untreated samples (Bahl OP, Mathur RB & Dhama TL, 1984).

375 Coagulation system activation is triggered by implanting blood contacting device-protein
376 interaction. The activation of factor XII is the first step in this activation process. Reciprocal as
377 well as auto activation will in turn cause the amplification of activated factor XII, where this will
378 initiate the intrinsic coagulation pathway through activation of factor XI, and finally lead to the
379 production of fibrin. Similarly, the activation of platelets by artificial surfaces occurs due to the
380 contact of platelets with artificial surfaces, in terms of ligand expression (GP IIb/IIIa).
381 Ultimately, these activated platelets either adhere to the surface of blood contacting devices
382 through proteins like fibrinogen or aggregate (Schopka et al, 2010). In order to function as a
383 viable blood contacting devices, the implanted blood contacting device should not elicit any
384 unwanted reactions leading to blood clot. In order to investigate that, the blood coagulation
385 assays were carried out in the mPE treated with HNO₃. There was a notable increase observed in
386 the PT and APTT of the HNO₃ treated mPE sample compared to the control. Changes in surface
387 morphology of mPE by acid treatment helped in improving the blood compatibility of the
388 polymers (Pandiyaraj et al, 2008). Thus, as discussed earlier, the increased PT and APTT is may
389 be attributed by improved surface roughness by the formation of nanotopographic surface by
390 HNO₃ on mPE.

391 This means that the surface modification of mPE with HNO₃ does not induce any damage
392 in erythrocytes' membranes that could lead to their lysis. Albeit some literatures indicate that it is
393 not possible to define a universal level of acceptable or unacceptable hemolysis values, a blood-
394 compatible material must inhibit hemolysis (Wenzhong et al, 2008). In this study, this parameter

395 is of extreme importance as the proposed mPE material will be in contact with blood for a
396 prolonged period in the blood circulation system.

397 The reduced platelet adhesion in the HNO₃ treated sample dictates the improved
398 hemocompatibility of surface modified mPE (Gomathi et al, 2012; Habibzadeh et al, 2014).
399 Hence, this modified mPE with more surface roughness, altered wettability, and better blood
400 compatibility may be the vital characteristics that can be utilized for construction of long-term
401 blood contacting devices like catheters, transvenous pacing leads, stents, grafts and etc.

402 **Conclusions**

403 The surface modification induced by HNO₃ on mPE and its effect on mPE blood
404 compatibility was assessed. Contact angle analysis depicts a decrease in the contact angle
405 elucidating increase in the wettability of the HNO₃ treated samples. There were no prominent
406 qualitative changes in the functional groups were observed by FTIR studies. The 3D Hirox
407 microscopy imaging also confirms the improved surface roughness by formation of more pits
408 and bumps in the acid treated sample than the control. SEM images of treated samples further
409 substantiate that acid treated sample surface possess more pits and pores compared to the control.
410 AFM topographical analysis shows an improved surface roughness in the 1 hour acid treated
411 sample compared to the control due to the etching effect of the acid. Blood coagulation assays
412 like PT and APTT ascertains a notable delay in the clotting mechanism on the surface of acid
413 treated samples. The result of hemolysis assay shows a minimum damage to red blood cells
414 (RBC). Platelet adhesion assay elucidates that the number of platelets adhered to the surface of
415 acid treated polymer was appreciably less in comparison to the untreated surface. The HNO₃
416 treatment of the mPE induces a surface modification in mPE and improves its porosity without

417 much effect on its tensile strength. Hence, HNO₃ treated mPE sample can be exploited for
418 various blood contacting biomaterial applications due to its improved blood compatibility.

419 **Acknowledgments**

420 This work was supported partly by GUP Universiti Teknologi Malaysia with the Grant
421 Vot No:Q.J130000.2509.10H13. The authors would like to thank MSI Technologies (M) Sdn.
422 Bhd and Progene director Mr.KH Ang for providing us KH-8700 3D Hirox Microscope for
423 imaging our samples and special thanks to Miss Farah Nadiya for helping us in assessing our
424 samples.

425 **References**

426 **Amarnath LP, Srinivas A, Ramamurthi A. 2006.** In vitro hemocompatibility testing of uv-
427 modified hyaluronan hydrogels. *Biomaterials* **27**:1416-1424 DOI
428 10.1016/j.biomaterials.2005.08.008.

429 **Bahl OP, Mathur RB and Dhama TL. 1984.** Effects of surface treatment on the mechanical
430 properties of carbon fibers. *Polymer Engineering & Science*, 24: 455–459. DOI
431 10.1002/pen.760240702.

432 **Cesca F, Limongi T, Accardo A, Rocchi A, Orlando M, Shalabaeva V, Fabrizio D,**
433 **Benfenati. 2014.** Fabrication of biocompatible free-standing nanopatterned films for primary
434 neuronal cultures. *RSC Advances* **4**:45696-45702 DOI 10.1039/C4RA08361J.

435 **Chau TT, Bruckard WJ, Koh PTL, Nguyen AV. 2009.** A review of factors that affect contact
436 angle and implications for flotation practice. *Advances in Colloid and Interface Science* **150**:
437 106-115 DOI 10.1016/j.cis.2009.07.003.

438 **Dong C, Eldawud R, Perhinschi G, Rojanasakul Y, Dinu CZ. 2013.** Effects of acid treatment
439 on structure, properties and biocompatibility of carbon nanotubes. *Applied Surface Science* **264**:
440 261–268 DOI 10.1016/j.apsusc.2012.09.180.

441 **Ferreira P, Coelho JFJ, Gil MH. 2008.** Development of a new photocrosslinkable
442 biodegradable bioadhesive. *International Journal of Pharmaceutics* **352**:172-181 DOI
443 10.1016/j.ijpharm.2007.10.026

444 **Formanek G, Frech RS. 1970.** Arterial thrombus formation during clinical percutaneous
445 catheterization. *Circulation* **41**:833–839 DOI 10.1161/01.CIR.41.5.833.

- 446 **Gomathi N, Rajasekar R, Babu RR, Mishrag D, Neogib S. 2012.** Development of bio/blood
447 compatible polypropylene through low pressure nitrogen plasma surface modification. *Materials*
448 *Science and Engineering: C* **32**:1767-1778 DOI 10.1016/j.msec.2012.04.034.
- 449 **Habibzadeh S, Li L, Shum-Tim D, Davis EC, Omanovic S. 2014.** Electrochemical polishing
450 as a 316l stainless steel surface treatment method: Towards the improvement of biocompatibility.
451 *Corrosion Science* **87**:89-100 DOI 10.1016/j.corsci.2014.06.010.
- 452 **Jaganathan SK, Mohandas H, Sivakumar G, Kasi P, Sudheer T, Veetil S. A, Murugesan S,**
453 **Supriyanto E. 2014a.** Enhanced blood compatibility of metallocene polyethylene subjected to
454 hydrochloric acid treatment for cardiovascular implants. *BioMed Research International* 1-7 DOI
455 10.1155/2014/459465.
- 456 **Jaganathan SK, Supriyanto E, Murugesan S, Balaji A, Asokan MK. 2014b.** Biomaterials in
457 *Cardiovascular Research: Applications and Clinical Implications.* *BioMed Research*
458 *International* 1-11 DOI 10.1155/2014/459465.
- 459 **John AA, Subramanian SP, Vellayappan MV, Balaji A, Jaganathan SK, Mohandas H,**
460 **Paramalinggam T, Supriyanto E, Yusof M. 2015.** Review: physico-chemical modification as a
461 versatile strategy for the biocompatibility enhancement of biomaterials. *RSC Advances* **5**:
462 39232-39244 DOI 10.1039/C5RA03018H.
463
- 464 **Kealy TJ, Pauson PL. 1951.** A new type of organo-iron compound. *Nature* 168:1039-1040 DOI
465 10.1038/1681039b0.
- 466 **Kwok SCH, Wang J, Chu PK. 2005.** Surface energy, wettability, and blood compatibility
467 phosphorus doped diamond-like carbon films. *Diamond and Related Materials* **14**:78-85 DOI
468 10.1016/j.diamond.2004.07.019.
- 469 **Li G, Zhang F, Liao Y, Yang P, and Huang N. 2010.** Coimmobilization of heparin/fibronectin
470 mixture on titanium surfaces and their blood compatibility. *Colloids Surf B Biointerfaces*
471 **81**:255-262 DOI 10.1016/j.colsurfb.2010.07.016.
- 472 **Ma G, Liu B, Li C, Huang D, Sheng J. 2012.** Plasma modification of polypropylene surfaces
473 and its alloying with styrene in situ. *Applied Surface Science* **258**:2424-2432 DOI
474 10.1016/j.apsusc.2011.10.065.
- 475 **Mohandas H, Sivakumar G, Kasi P, Jaganathan SK, Supriyanto E. 2013.** Microwave-
476 assisted surface modification of metallocene polyethylene for improving blood compatibility.
477 *BioMed Research International* 21-7 DOI 10.1155/2013/253473.
- 478 **Moreno-Castilla C, Ferro-Garcia MA, Joly JP, Bautista-Toledo I, Carrasco-Marin F,**
479 **Rivera-Utrilla J. 1995.** Activated carbon surface modifications by nitric acid, hydrogen

- 480 peroxide, and ammonium peroxydisulfate treatments. Langmuir: the ACS journal of surfaces and
481 colloids 4386-4392 DOI 10.1021/la00011a035
- 482 **Pelagade SM, Rane RS, Mukherjee S, Deshpande UP, Ganesan V, Shripathi T. 2012.**
483 Investigation of surface free energy for ptfе polymer by bipolar argon plasma treatment. Journal
484 of Surface Engineered Materials and Advanced Technology 2:132-136 DOI
485 10.4236/jsemat.2012.22021
- 486 **Pereira C, Busani T, Branco LC, Joosten I, Sandu IC. 2013.** Nondestructive characterization
487 and enzyme cleaning of painted surfaces: Assessment from the macro to nano level. Microscopy
488 and Microanalysis 19:1632-1644 DOI 10.1017/S1431927613013196
- 489 **Pandiyaraj KN, Selvarajan V, Rhee YH, Kim HW, Shah SI. 2009.** Glow discharge plasma-
490 induced immobilization of heparin and insulin on polyethylene terephthalate film surfaces
491 enhances anti-thrombogenic properties. Materials Science and Engineering: C 29:796-805 DOI
492 10.1016/j.msec.2008.07.013.
- 493 **Qi P, Maitz MF, Huang N. 2013.** Surface modification of cardiovascular materials and
494 implants. Surface and Coatings Technology 233:80-90 DOI 10.1016/j.surfcoat.2013.02.008
- 495 **Schopka S, Schmid T, Schmid C, Lehle K. 2010.** Current strategies in cardiovascular
496 biomaterial functionalization. Materials 3:638-655 DOI 10.3390/ma3010638.
- 497 **Slepicka P, Kasálková N, Slepcková N, Stránská E, Bacáková L, Švorcík V. 2013.** Surface
498 characterization of plasma treated polymers for applications as biocompatible carriers. EXPRESS
499 Polymer Letters 7:535-545 DOI 10.3144/expresspolymlett.2013.50.
- 500 **Thompson. 2013.** M. Medtech Insight Reports.
- 501 **Tverdokhlebov SI, Bolbasov EN, Shesterikov EV, Antonovab LV, Golovkinb AS, Matveeva**
502 **VG, Petlin DG, Anissimov YG. 2015.** Modification of polylactic acid surface using rf plasma
503 discharge with sputter deposition of a hydroxyapatite target for increased biocompatibility.
504 Applied Surface Science 329:32-39 DOI 10.1016/j.apsusc.2014.12.127.
- 505 Vascular Access 2006 Work Group. 2006. American Journal of Kidney Diseases 176-S247.
- 506 **Vital A, Vayer M, Sinturel C, Tillocher T, Lefauchaux P, Dussart R. 2015.** Polymer masks
507 for structured surface and plasma etching. Applied Surface Science 332:237-246 DOI
508 10.1016/j.apsusc.2015.01.040.
- 509 **Vellayappan MV, Balaji A, Subramanian AP, John AA, Jaganathan SK, Murugesan S,**
510 **Supriyanto E, Mustafa Y. 2015a.** Multifaceted prospects of nanocomposites for cardiovascular
511 grafts and stents. International Journal of Nanomedicine 10:2785—2803.

512 **Vellayappan MV, Balaji A, Subramanian AP, John AA, Jaganathan SK, Murugesan S,**
513 **Hemanth S, Supriyanto E, Mustafa Y. 2015b.** Tangible nanocomposites with diverse
514 properties for heart valve application. *Science and Technology of Advanced Materials* 16: 1-18
515 DOI 10.1088/1468-6996/16/3/033504.

516 **Wanke CH, Feijó JL, Barbosa LG, Campo LF, Oliveira RVB, Horowitz F. 2011.** Tuning of
517 polypropylene wettability by plasma and polyhedral oligomeric silsesquioxane modifications.
518 *Polymer* 52:1797-1802 DOI 10.1016/j.polymer.2011.01.064.

519 **Wenzhong S, Li, Liu Z, Yihong. 2008.** Surface chemical functional groups modification of
520 porous carbon. *Recent Patents on Chemical Engineering* 1:27-40 DOI
521 10.2174/2211334710801010027.

522 **Xu Q, Yang Y, Yang J, Wang X, Wang Z, Wang Y. 2013.** Plasma activation of porous
523 polytetrafluoroethylene membranes for superior hydrophilicity and separation performances via
524 atomic layer deposition of tio_2 . *Journal of Membrane Science* 443:62-68 DOI
525 10.1016/j.memsci.2013.04.061.

526 **Yue M, Zhou B, Jiao K, Qiana X, Xua Z, Tenga K, Zhaoa L, Wang J, Jiao Y. 2015.**
527 Switchable hydrophobic/hydrophilic surface of electrospun poly (l-lactide) membranes obtained
528 by cf_4 microwave plasma treatment. *Applied Surface Science* 327:93-99 DOI
529 10.1016/j.apsusc.2014.11.149.

530 **Zhang Y, Zhu S, Liu Y, Yang Band Wang X. 2014.** The mechanical and tribological
531 properties of nitric acid-treated carbon fiber-reinforced polyoxymethylene composites. *Journal of*
532 *Applied Polymer Science* 132:41812 DOI 10.1002/app.41812

533 **Zhao T, Li Y, Gao Y, Xiang Y, Chen H, Zhang T, 2011.** Hemocompatibility investigation of
534 the niti alloy implanted with tantalum. *Journal of Materials Science: Materials in Medicine* 22:
535 2311-2318 DOI 10.1007/s10856-011-4406-4.

536

537

538

539

540

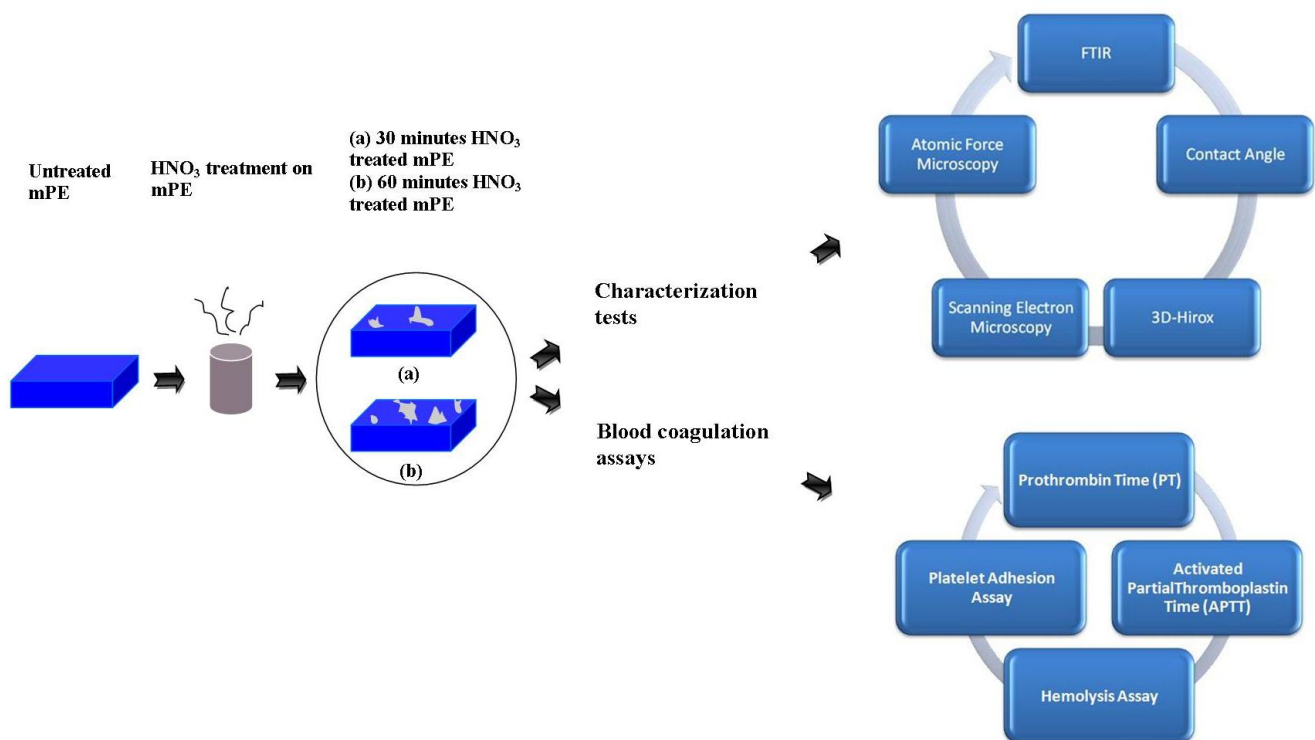
541

542

543

544

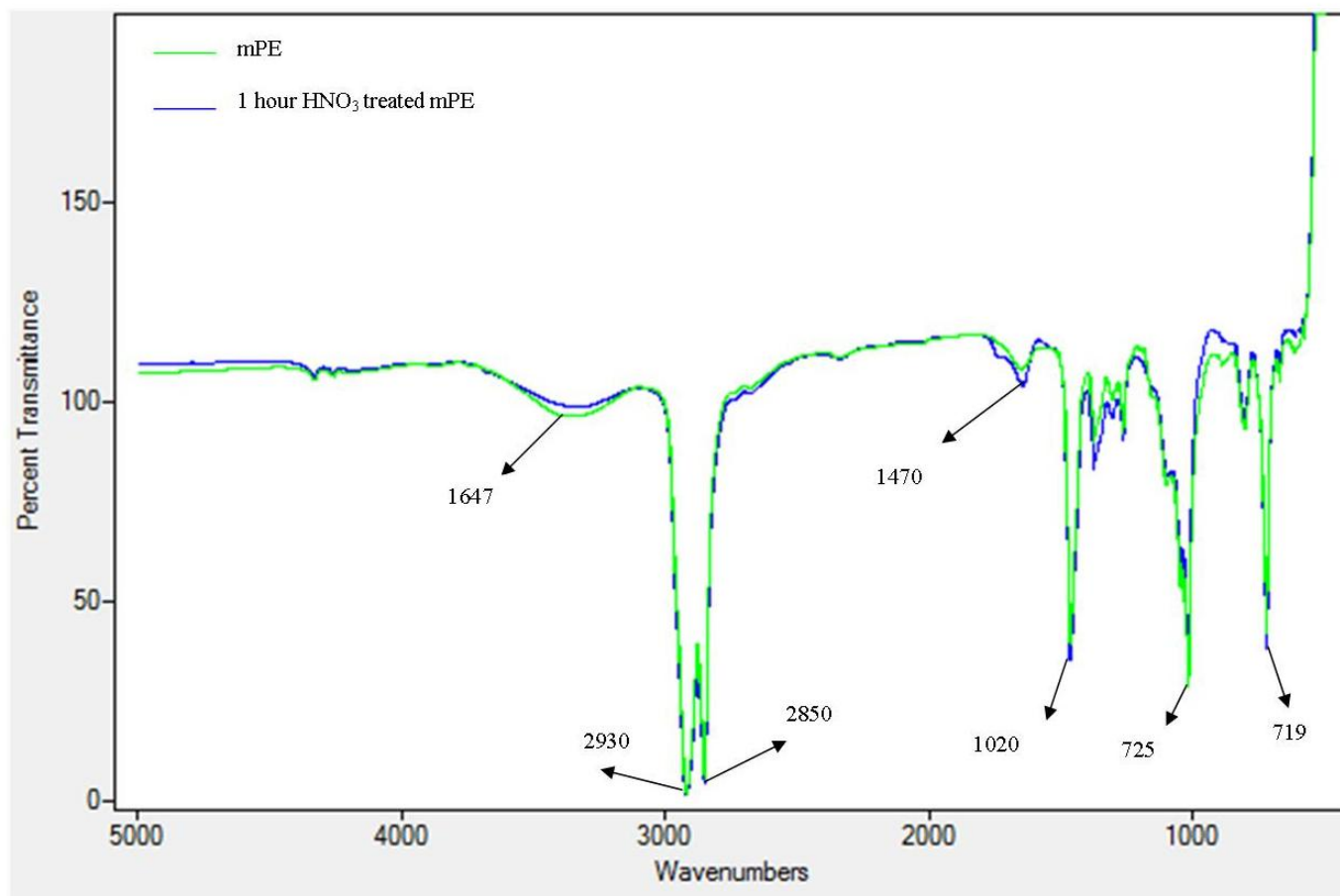
545
 546
 547
 548
 549
 550



551
 552
 553
 554
 555
 556
 557
 558
 559
 560
 561
 562
 563
 564

Figure 1 Schematic representation of series of characterization and blood compatibility experiments done

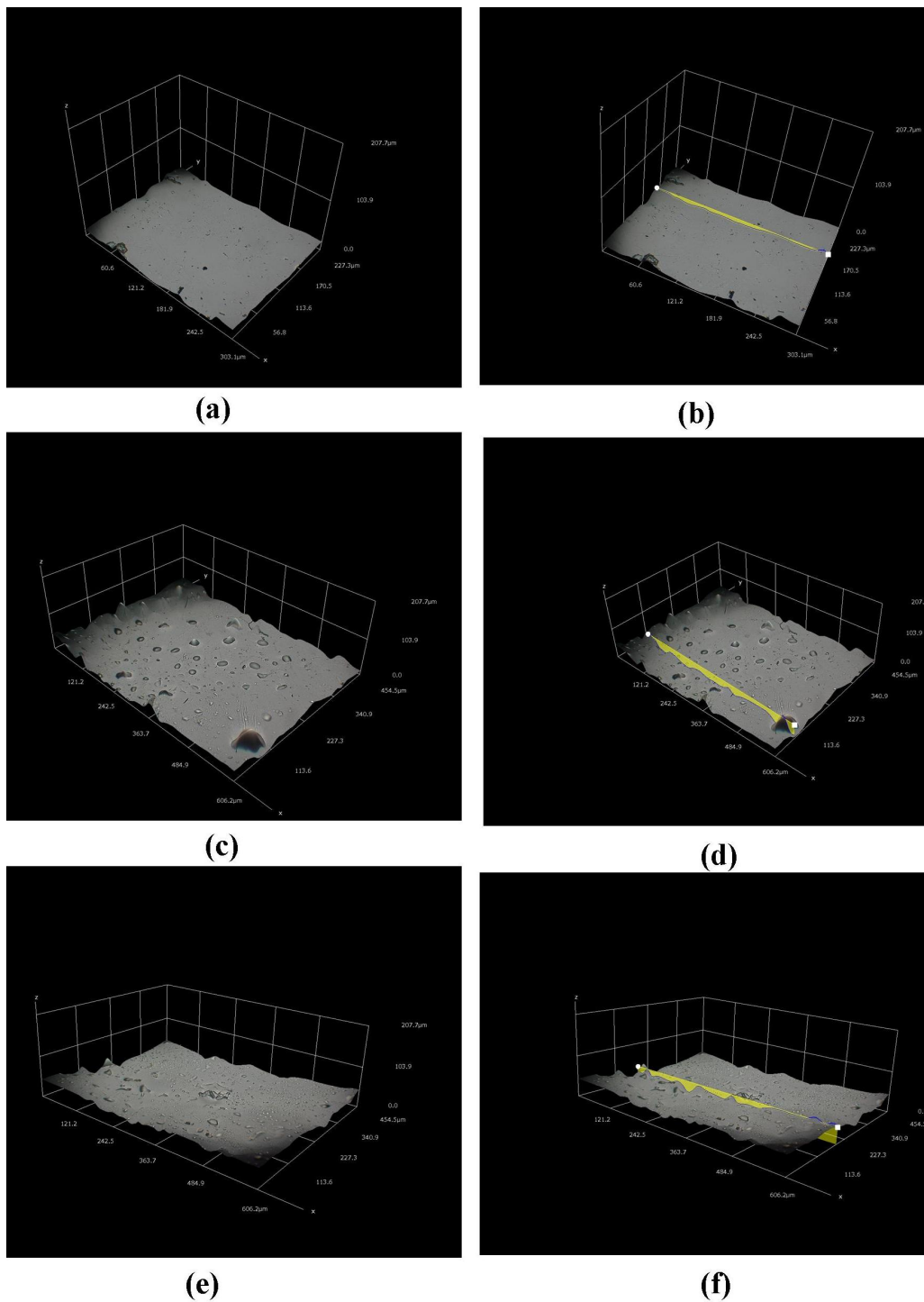
565
566
567
568
569



570
571
572
573
574
575
576
577
578

579 **Figure 2** A representative FTIR spectra of untreated and 60 min HNO₃-treated metallocene
580 polyethylene

581
582
583
584
585
586
587
588
589
590
591
592
593
594
595
596
597
598
599
600
601
602
603
604
605
606
607
608
609
610
611



612 **Figure 3** Different three-dimensional representations using 3D Hirox digital microscopy (a)
613 Untreated mPE (b) Untreated mPE with profiling (c) 30 minutes HNO_3 treated mPE (d) 30
614 minutes HNO_3 treated mPE profiling (e) 60 minutes HNO_3 treated mPE (e) 60 minutes HNO_3
615 treated mPE profiling

616

617

618

619

620

621

622

623

624

625

626

627

628

629

630

631

632

633

634

635

636

637

638

639

640

641

642

643

644

645

646

647

648

649

650

651

652

653

654

655

656

657

658

659

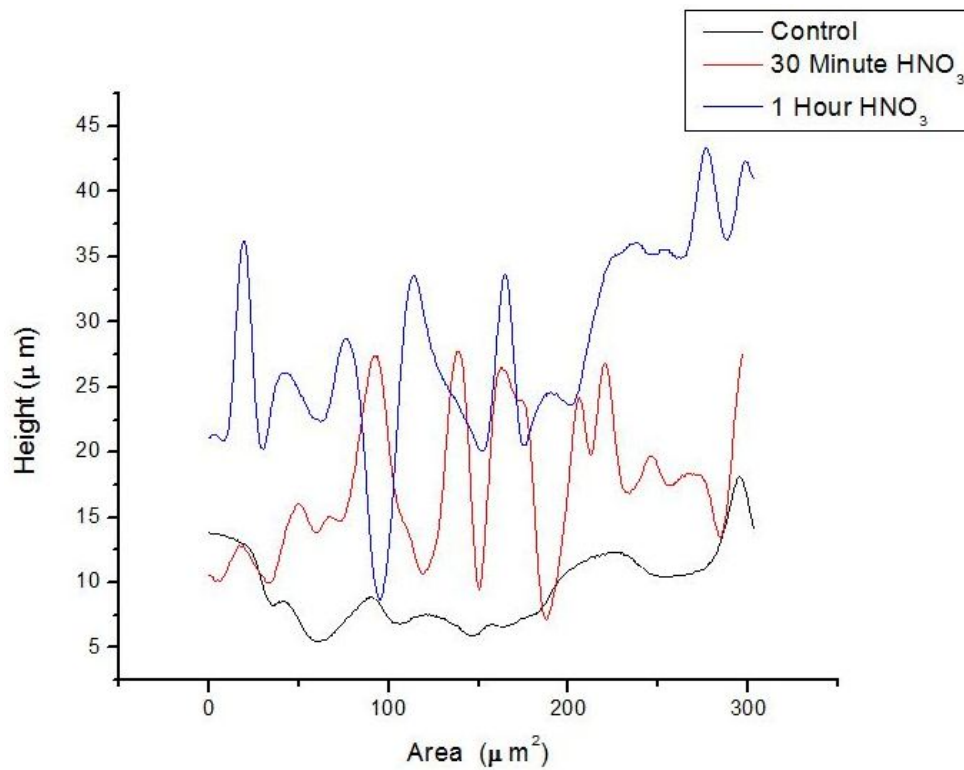
660

661

662

663

664



652 **Figure 4** The representative height of the pores of different samples measured using 3D-
653 profiling of 3D Hirox digital microscopy

654

655

656

657

658

659

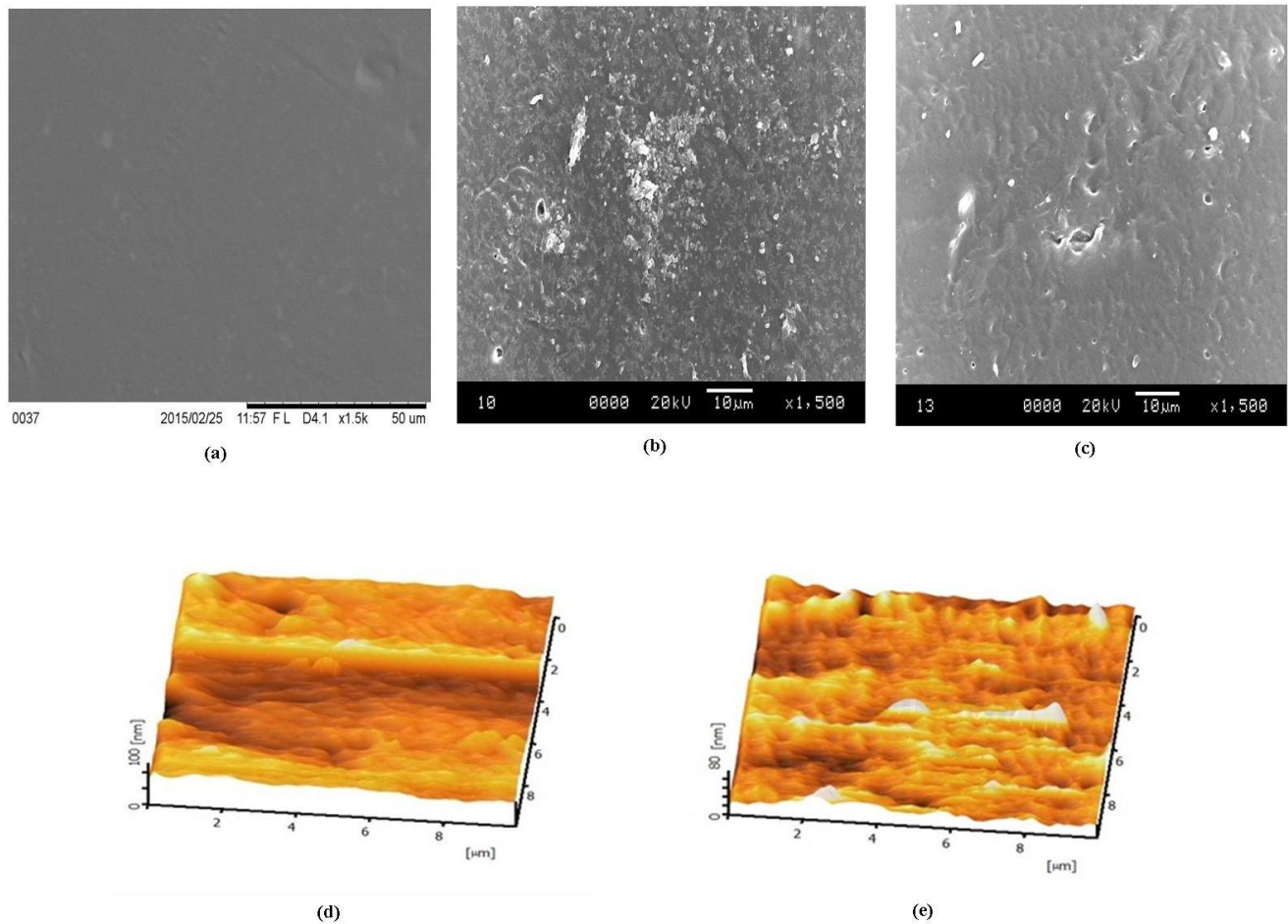
660

661

662

663

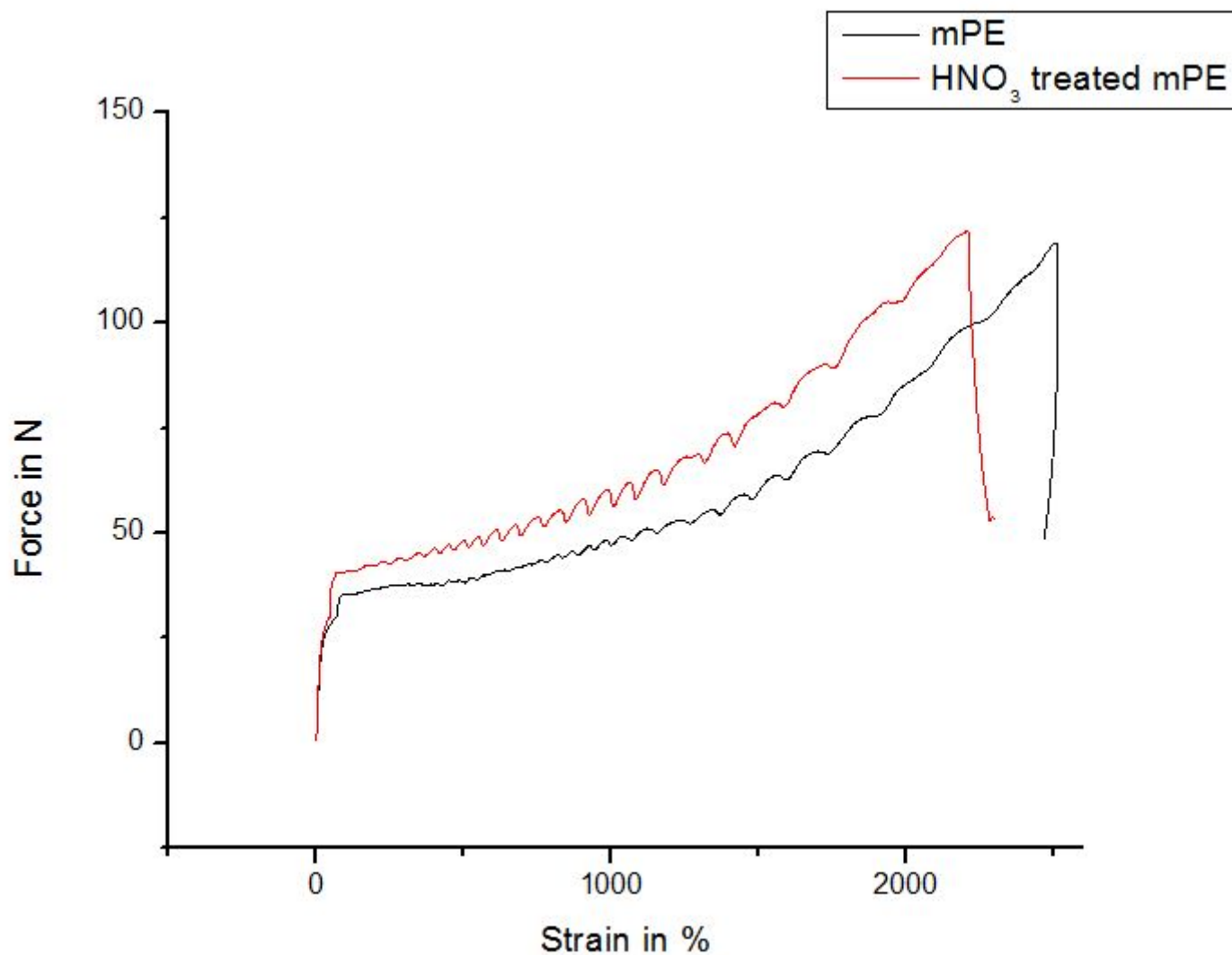
664



665
 666
 667
 668
 669
 670
 671 **Figure 5** (a), (b) and (c) are representative SEM micrographs of untreated and HNO₃ treated
 672 metalocene polyethylene. Here, (d) and (e) are representative AFM images of untreated
 673 metalocene polyethylene and one hour HNO₃ treated metalocene polyethylene respectively

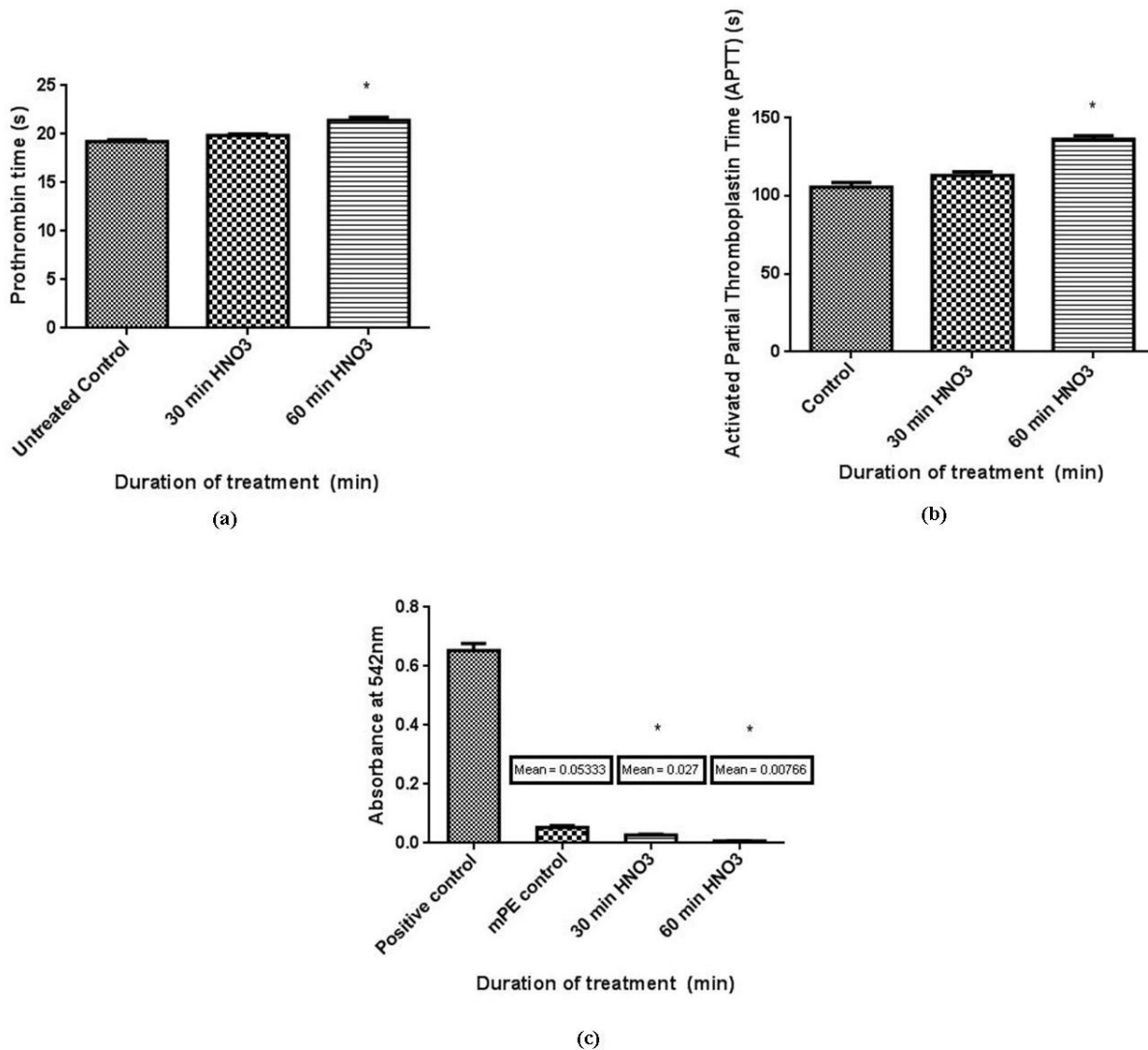
674
 675
 676
 677
 678
 679
 680
 681
 682
 683
 684
 685
 686
 687

688
689
690
691



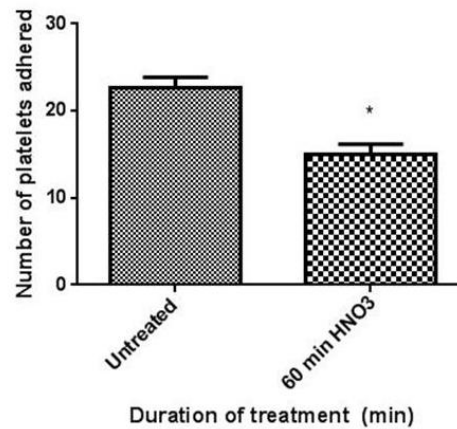
692
693
694
695
696
697
698
699
700
701

Figure 6 Tensile testing result of mPE before and after nitric acid treatment

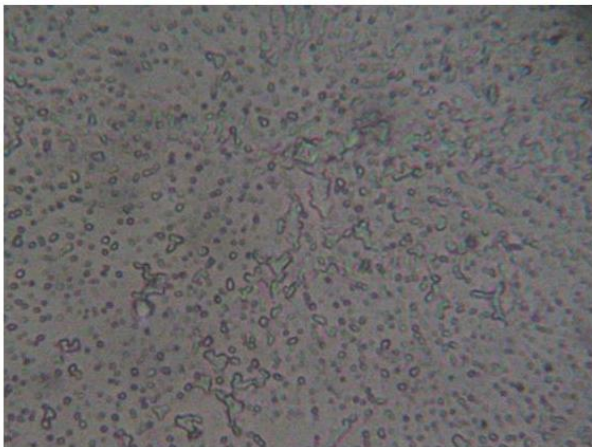


702
 703
 704
 705
 706
 707
 708
 709
 710
 711
 712
 713
 714
 715
 716

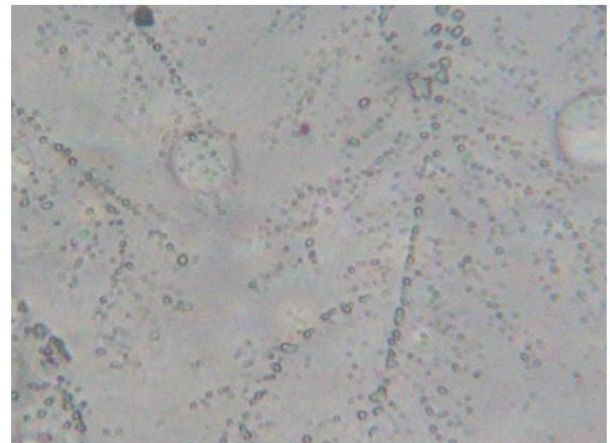
Figure 7 (a) Comparison of prothrombin time (PT) of control and HNO₃-treated metalocene polyethylene ($n = 3$) (b) The activated partial thromboplastin time (APPT) of control and HNO₃-treated metalocene polyethylene ($n = 3$) (c) The absorbance of control and HNO₃-treated metalocene polyethylene ($n = 3$) for all three panels, values shown are mean \pm SD and * indicating differences in the mean are significant ($P < 0.05$)



(a)



(b)



(c)

717
718
719
720
721
722
723
724
725
726
727
728
729
730
731
732

Figure 8 Platelet adhesion assay of untreated and HNO₃-treated metalocene polyethylene ($n = 3$), a shows the number of platelets adhered on the untreated and 60 min HNO₃ exposed surface and values are expressed as mean \pm SD. * Differences in the means are significant with $P < 0.05$. Figure b and c delineates photomicrograph of platelets adhered on untreated and 60 min HNO₃-treated mPE at 40x magnification

733

734 **Table 1** Contact angle measurement of the mPE before and after HNO₃ treatment

735

S. No	Sample	Average contact angle in degrees*
1	Untreated mPE	86.06±1.15
2	mPE treated with HNO ₃ (30 min)	72.03±2.05
3	mPE treated with HNO ₃ (60 min)	69.73±1.41

736

737

738

739

740 **Table 2** Tensile testing result of mPE before and after 1 hour nitric acid treatment

741

S. No	Sample	E-Modulus MPa	Fmax. N	E-FMax.%	W up to Fmax.Nmm
1	Untreated mPE	31.32	119.09	2510.82	30680.25
2	mPE treated with HNO ₃ (60 min)	34.75	121.85	2510.39	32513.68

742

743